

X-ray scattering of thin liquid films: Beyond the harmonic approximation

Ming Li*

Institute of Physics and Center for Condensed Matter Physics, Chinese Academy of Sciences, Beijing 100080, People's Republic of China

Mark L. Schlossman†

Department of Physics and Department of Chemistry, University of Illinois, Chicago, Illinois 60607

(Received 27 February 2002; published 25 June 2002)

We calculate the x-ray scattering from coupled capillary fluctuations of thin liquid films, taking into account an asymmetric interfacial interaction potential. Harmonic expansion of the potential around its minimum produces the well-known Kiessig fringes in both specular reflectivity and longitudinal diffuse scattering. The addition of a cubic term to the expansion, representing the asymmetry, leads to q_z -dependent changes of the modulation period of the Kiessig fringes. The cubic term produces a relative phase shift between the interference fringes of the specular reflectivity and the off-specular longitudinal diffuse scattering. It is suggested that these effects may be used to estimate, via x-ray scattering, the interfacial potential of thin liquid films.

DOI: 10.1103/PhysRevE.65.061608

PACS number(s): 68.15.+e, 68.05.-n, 61.10.-i

I. INTRODUCTION

Thin liquid films are of interest for practical, as well as theoretical, reasons. They are very important in many technological and biological processes such as flotation, tertiary oil recovery, biological cell interaction and fusion, spreading of fluids in coating, and other similar processes involving moving contact lines, selective etching, and forming and protecting chips and microsensors in the microelectronics industry, among others [1]. The thermodynamics of the films is determined by the interfacial interactions [2]. A model for the free-energy F (per unit area) of a film of thickness l is $F(l) = \gamma_1 + \gamma_2 + \Delta G(l)$, where γ_j ($j=1,2$) are the interfacial tensions of the two interfacial boundaries of the film [3]. For large l , $\Delta G(l)$ tends toward zero. The interfacial potential or excess interfacial free energy $\Delta G(l)$ can often be approximated as consisting of a short-range force and a long-range van der Waals interaction, written as [4,5]

$$\Delta G(l) = S_p e^{-l/\Lambda} - A/12\pi l^2, \quad (1.1)$$

where S_p is the amplitude of the short-range interaction, A is an effective Hamaker constant (Fig. 1). The first term in Eq. (1.1) models a short-range interaction with decay length Λ [6], and the second term is the van der Waals interaction between two planar interfaces, separated by a distance l . In some cases it is necessary to add a higher-order term proportional to l^{-3} to the van der Waals interaction [7]. Different approaches have been used to study the interfacial potential. The disjoining pressure, $\Pi = \partial \Delta G / \partial l$, can be measured as a function of thickness of the films [2,8–10]. This is practical for free-standing liquid films and for films confined between two solid surfaces. Ellipsometry, contact angle, and adsorption measurements have been used to study the wetting of thin liquid films on both solid and liquid substrates (for a review, see [11]). X-ray studies have measured the interac-

tion of thin films on top of solid surfaces [12,13], and of thin liquid films on top of liquid subphases [14].

Numerous x-ray scattering measurements have demonstrated the suitability of capillary wave theory to describe fluctuations of liquid interfaces and their interactions [13–17]. For example, for a complete wetting layer on a solid surface, the thermal fluctuations on the surface are confined by the substrate via a long-range interaction. By carefully measuring the confinement as a function of thickness, one can estimate the Hamaker constant of the system [12]. We recently used x-ray scattering and interfacial tension measurements to study the interfacial potential in thin liquid films on top of a liquid subphase [14]. In the present work we calculate, via functional integrals, the x-ray scattering from coupled capillary fluctuations of thin liquid films, taking into account the asymmetric feature of the profile of the interfacial interaction potential. It is shown that the interference terms of the Kiessig fringes of both the specular reflectivity and the longitudinal diffuse scattering are q_z dependent. We demonstrate that there is a relative phase shift between the interference fringes of the specular reflectivity and the off-specular longitudinal diffuse scattering. This may provide a useful experimental signature for determining the asymmetric shape of the interfacial interaction potential.

The mean thickness, l_m , of a partial wetting layer is kept constant by the disjoining pressure, which acts as the restor-

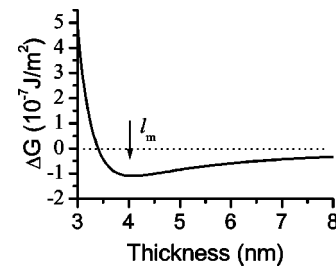


FIG. 1. An example of the interfacial potential calculated for $S_p = 18.8 \times 10^{-3} \text{ J/m}^2$, $A = 8.0 \times 10^{-23} \text{ J}$, and $\Lambda = 0.295 \text{ nm}$. For this potential, one can calculate the coupling parameter $B = 1.66 \times 10^{11} \text{ J/m}^4$, the phase shift parameter $C = 6.72 \times 10^{20} \text{ J/m}^5$, and the film thickness $l_m = 4.08 \text{ nm}$.

*Email address: mingli@aphy.iphys.ac.cn

†Email address: schloss@uic.edu

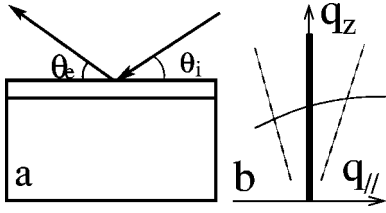


FIG. 2. (a) Geometry of x-ray scattering from a thin film. (b) Three scanning modes described in the text. Thick vertical line: specular reflectivity. Dashed lines: longitudinal diffuse scattering. Solid curve: transverse diffuse scattering.

ing force to thermal fluctuations. The first derivative of $\Delta G(l)$ vanishes at this thickness. The interplay between the short- and long-range interactions creates a strong dynamical coupling between the capillary waves on the two interfaces. The second derivative of $\Delta G(l)$ measures the strength of this coupling. If one expands the potential to second order, the correlation functions of the capillary waves can be easily calculated by Gaussian functional integration [14,18]. In this approximation, the shape of the potential near its minimum is presumably symmetric. However, the real interaction potential is expected to be asymmetric. By expanding $\Delta G(l)$ to third order, we shall show that the asymmetry leads to a q_z -dependent variation of the modulation period of the Keesig fringes.

II. THEORY

A. X-ray scattering of thin liquid films

Figure 2 sketches the x-ray scattering geometry from a thin liquid film. The scattering function, which is proportional to the observed intensity at point (q_{\parallel}, q_z) in reciprocal space, can be expressed as [19,20]

$$S(q_{\parallel}, q_z) = \sum_{j=1,2} \frac{\Delta \rho_j^2}{q_z^2} \int d^2r \langle e^{iq_z[\xi_j(r) - \xi_j(0)]} \rangle e^{iq_{\parallel}r} + \frac{\Delta \rho_1 \Delta \rho_2}{q_z^2} \int d^2r [e^{iq_z l_m} \langle e^{iq_z[\xi_1(r) - \xi_2(0)]} \rangle + \text{c.c.}] e^{iq_{\parallel}r}, \quad (2.1)$$

where $\Delta \rho_j$ is the difference in electron density across interface j ; $\xi_j(r)$ is the local interfacial height of the sharp interface above the mean interfacial plane j ; r is the displacement between two points on the interfaces; $\langle \dots \rangle$ represents the canonical average; and c.c. refers to the complex conjugate. In the literature, it is generally assumed that the fluctuations satisfy a Gaussian distribution [19]. Thus, the correlation functions (described below) are all real. We will show in the next section that this corresponds to the assumption that the potential in Eq. (1.1) is parabolic near its minimum. If one goes a step further to take into account the cubic term, the cross-correlation function is complex.

When $q_{\parallel} = 0$, one measures the reflectivity of the thin films. This is realized by scanning the incident angle θ_i and the exit angle θ_e simultaneously while keeping $\theta_i = \theta_e$ [21]. The period of the interference fringes is determined by the

film thickness l_m , namely, by $\cos(q_z l_m)$. If $q_{\parallel} \neq 0$, one measures diffuse scattering from the interfacial fluctuations of thin films. This can be realized in several ways (see Fig. 2). (i) Longitudinal diffuse scattering measured either by scanning θ_i and θ_e simultaneously while keeping $\theta_i = \theta_e + \Delta \theta$ (as shown in Fig. 2), or by scanning q_z with a constant offset in q_{\parallel} . If the capillary wave fluctuations of the two interfaces are correlated, one measures interference fringes as a function of q_z , similar to that in the specular reflectivity. (ii) Transverse diffuse scattering measured by scanning θ_i or θ_e alone while keeping θ_e or θ_i constant (experimentally, this is convenient, though not exactly transverse to the specular reflectivity). The shape of the transverse diffuse scattering intensity is determined by the spectra of the two interfacial capillary waves, as well as by cross-correlations in the fluctuations between the two interfaces of the film.

B. The correlation functions

The correlation functions are determined by an analysis of the capillary-wave Hamiltonian. In this model, the interfacial width is the result of capillary-wave roughening of a sharp interface. The range in \mathbf{q} space of our previously reported experiment does not justify the use of more complicated models of the interfaces [14,17]. Here, we modify the standard capillary-wave Hamiltonian to account for the interfacial interaction [14]. A Taylor expansion about the minimum l_m of the excess interfacial free energy $\Delta G(l)$ (see Fig. 1) yields $\Delta G(l) \approx -A + \frac{1}{2}B(l - l_m)^2 - \frac{1}{6}C(l - l_m)^3$ (note that $\partial \Delta G / \partial l = 0$ at the minimum). Adding the energy of thermal fluctuations to the free energy, one has the Hamiltonian of the system per unit area,

$$H_{total} = \frac{1}{A_0} \int d^2r \{ \gamma_1 [1 + \frac{1}{2}(\nabla \xi_1)^2] + \gamma_2 [1 + \frac{1}{2}(\nabla \xi_2)^2] + b(\xi_1 - \xi_2)^2 - c(\xi_1 - \xi_2)^3 \}, \quad (2.2)$$

where $b = B/2$, $c = C/6$, A_0 is the interfacial area, and γ_i ($i = 1, 2$) is the interfacial tension of interface i . Here, only the local interaction of the interfaces has been taken into account (the Derjaguin approximation [22,23]). It is a good approximation when $q_{\parallel} < 1/l_m$ [23], which is practically satisfied in our reported x-ray experiment [14]. Also, we have ignored the effect of gravitation, which can be accounted for by introducing a long wavelength cutoff [18,24]. Substituting $\eta = \xi_1 - \xi_2$ and $\zeta = \gamma_1 \xi_1 + \gamma_2 \xi_2$, Eq. (2.2) is rewritten as

$$H_{total} = \frac{1}{A_0} \int d^2r \{ a'(\nabla \zeta)^2 + a(\nabla \eta)^2 + b\eta^2 - c\eta^3 \}, \quad (2.3)$$

where $a' = 1/(2\gamma_1 + 2\gamma_2)$ and $a = \gamma_1 \gamma_2 / (2\gamma_1 + 2\gamma_2)$. Since ξ_j is the local height or fluctuation of interface j above the mean position of interface j , η is the difference in the fluctuations of the two interfaces. If the local thickness of the film remains constant throughout the film, then $\eta = 0$. Now the Hamiltonian consists of two parts that are independent of each other. Therefore, the correlation functions take the forms

$$\begin{aligned} & \langle \exp\{iq_z[\xi_1(r_1) - \xi_1(r_2)]\} \rangle \\ &= \left\langle \exp\left\{iq_z\left(\frac{\zeta(r_1) - \zeta(r_2)}{\gamma_1 + \gamma_2}\right)\right\} \right\rangle \\ & \times \left\langle \exp\left\{iq_z\left(\frac{\gamma_2}{\gamma_1 + \gamma_2}\right)[\eta(r_1) - \eta(r_2)]\right\} \right\rangle, \end{aligned} \quad (2.4a)$$

$$\begin{aligned} & \langle \exp\{iq_z[\xi_2(r_1) - \xi_2(r_2)]\} \rangle \\ &= \left\langle \exp\left\{iq_z\left(\frac{\zeta(r_1) - \zeta(r_2)}{\gamma_1 + \gamma_2}\right)\right\} \right\rangle \\ & \times \left\langle \exp\left\{-iq_z\left(\frac{\gamma_1}{\gamma_1 + \gamma_2}\right)[\eta(r_1) - \eta(r_2)]\right\} \right\rangle, \end{aligned} \quad (2.4b)$$

$$\begin{aligned} & \langle \exp\{iq_z[\xi_1(r_1) - \xi_2(r_2)]\} \rangle \\ &= \left\langle \exp\left\{iq_z\left(\frac{\zeta(r_1) - \zeta(r_2)}{\gamma_1 + \gamma_2}\right)\right\} \right\rangle \\ & \times \left\langle \exp\left\{iq_z\left(\frac{\gamma_2\eta(r_1) + \gamma_1\eta(r_2)}{\gamma_1 + \gamma_2}\right)\right\} \right\rangle. \end{aligned} \quad (2.4c)$$

The first parts on the right-hand sides of Eqs. (2.4) are real functions and will be considered in the next section. To calculate the second parts on the right-hand sides of Eqs. (2.4), we consider the Hamiltonian

$$H = \int d^2r \{a(\nabla\eta)^2 + b\eta^2 - c\eta^3\}, \quad (2.5)$$

and denote it as H_0 when $c=0$. The technique of functional integration, as used in field theory, allows us to calculate the correlation functions in Eqs. (2.4) when c is small and the term $c\eta^3$ is treated perturbatively. Following Zinn-Justin, we consider the Gaussian functional integral [25]

$$Z(J) = \int [d\eta] e^{\beta c \int d^2r \eta^3} e^{-(1/2)\eta K \eta + J\eta}, \quad (2.6)$$

where the kernel $K(r, w) = (-2a\beta\nabla^2 + 2b\beta)\delta^2(r-w)$, with $\beta = 1/k_B T$, $\eta K \eta = \int d^2r \eta(r) K(r, w) \eta(w) d^2w$, and $J\eta = \int d^2r J(r) \eta(r)$. Using the property of a functional derivative $(\delta/\delta J)e^{J\eta} = \eta e^{J\eta}$, we have

$$\begin{aligned} Z(J) &= e^{\beta c \int d^2r (\delta/\delta J)^3} \int [d\eta] e^{-(1/2)\eta K \eta + J\eta} \\ &\approx \left[1 + \beta c \int d^2r \left(\frac{\delta}{\delta J}\right)^3 \right] e^{(1/2)J\Xi J}, \end{aligned} \quad (2.7)$$

where $\Xi(r, w)$ is the inverse kernel that takes the form [25]

$$\Xi(r, w) = \int_{-\infty}^{\infty} \frac{d^2p}{(2\pi)^2} \frac{e^{ip(r-w)}}{2a\beta p^2 + 2b\beta}, \quad (2.8)$$

and satisfies $\int d^2v \Xi(r, v) K(v, w) = \delta^2(r-w)$. Note that $J\Xi J = \int d^2r d^2w J(r) \Xi(r, w) J(w)$. Also,

$$\left\langle \exp\left\{iq_z\left(\frac{\gamma_1\eta(r_2) + \gamma_2\eta(r_1)}{\gamma_1 + \gamma_2}\right)\right\} \right\rangle = e^{\hat{O}Z(J)}|_{J=0}, \quad (2.9)$$

with the operator

$$\hat{O} = \frac{iq_z}{\gamma_1 + \gamma_2} \left(\gamma_2 \frac{\delta}{\delta J(r_1)} + \gamma_1 \frac{\delta}{\delta J(r_2)} \right). \quad (2.10)$$

The integrand in Eq. (2.7) is

$$\begin{aligned} & \left(\frac{\delta}{\delta J}\right)^3 e^{1/2 J\Xi J} = 3\Xi(r, r) e^{(1/2)J\Xi J} \left(\frac{1}{2}\Xi J + \frac{1}{2}J\Xi\right) \\ & + e^{(1/2)J\Xi J} \left(\frac{1}{2}\Xi J + \frac{1}{2}J\Xi\right)^3, \end{aligned} \quad (2.11)$$

where the conventions $\Xi J = \int d^2w \Xi(r, w) J(w)$ and $J\Xi = \int d^2w J(w) \Xi(w, r)$ have been used. The first term leads to an increase in the film thickness of $\Delta l = 3c\Xi(0,0)/4b$, similar to the thermal expansion of a crystal that results from anharmonic interactions. In the present case, the absolute value of the film thickness is not a direct experimental signature for the presence of anharmonic interactions because other aspects of the interaction can modify the thickness. For example, adding a term such as $\int d^2r 3c\Xi(0,0)\eta(r)$ to the Hamiltonian would result in the same effect. Here, we focus our attention on the second term in Eq. (2.11), which leads to an experimental signature of the anharmonic term. Applying the operator $e^{\hat{O}}$ to this term, we have

$$\begin{aligned} & e^{\hat{O}} \left(\frac{1}{2}\Xi J + \frac{1}{2}J\Xi\right)^3 e^{(1/2)J\Xi J} \Big|_{J=0} \\ &= \frac{\hat{O}^3 \left(\frac{1}{2}\Xi J + \frac{1}{2}J\Xi\right)^3}{6} \Big|_{J=0} e^{\hat{O}} e^{(1/2)J\Xi J} \Big|_{J=0}. \end{aligned} \quad (2.12)$$

Combining this with Eqs. (2.7) and (2.9), we have

$$\begin{aligned} & \left\langle \exp\left\{iq_z\left(\frac{\gamma_1\eta(r_2) + \gamma_2\eta(r_1)}{\gamma_1 + \gamma_2}\right)\right\} \right\rangle \\ &= \left(1 - \frac{iq_z^3 \beta c}{8(\gamma_1 + \gamma_2)^3} \int d^2r \{ \gamma_2 [\Xi(r, r_1) + \Xi(r_1, r)] \right. \\ & \quad \left. + \gamma_1 [\Xi(r, r_2) + \Xi(r_2, r)] \}^3 \right) \\ & \times \left\langle \exp\left\{iq_z\left(\frac{\gamma_1\eta(r_2) + \gamma_2\eta(r_1)}{\gamma_1 + \gamma_2}\right)\right\} \right\rangle_{H_0}, \end{aligned} \quad (2.13)$$

where the subscript H_0 represents the canonical average when $c=0$. A similar process leads to

$$\begin{aligned} & \left\langle \exp \left\{ \pm i q_z \left(\frac{\gamma_{2,1}}{\gamma_1 + \gamma_2} \right) [\eta(r_1) - \eta(r_2)] \right\} \right\rangle \\ &= \left\langle \exp \left\{ \pm i q_z \left(\frac{\gamma_{2,1}}{\gamma_1 + \gamma_2} \right) [\eta(r_1) - \eta(r_2)] \right\} \right\rangle_{H_0}. \end{aligned} \quad (2.14)$$

Thus, the correlation functions in Eqs. (2.4a) and (2.4b) are real, and the correlation function in Eq. (2.4c) is complex. Substituting these functions into Eq. (2.1), one can see that the scattering from the two individual interfaces is not affected by the asymmetry of the interaction potential; but the interference effect, due to the cross-correlation function, depends on both the quadratic and cubic terms of the Taylor expansion of the potential.

III. RESULTS

Using the definition in Eq. (2.8) to calculate the integration in Eq. (2.13), we have

$$\begin{aligned} & \left\langle \exp \left\{ i q_z \left(\frac{\gamma_1 \eta(r_2) + \gamma_2 \eta(r_1)}{\gamma_1 + \gamma_2} \right) \right\} \right\rangle \\ &= \{1 - i q_z^3 [\Phi_0 + \Phi(r_1 - r_2)]\} \\ & \times \left\langle \exp \left\{ i q_z \left(\frac{\gamma_1 \eta(r_2) + \gamma_2 \eta(r_1)}{\gamma_1 + \gamma_2} \right) \right\} \right\rangle_{H_0}, \end{aligned} \quad (3.1)$$

where

$$\begin{aligned} \Phi_0 &= \frac{\beta c}{(\gamma_1 + \gamma_2)^3} \frac{\gamma_1^3 + \gamma_2^3}{(2\pi)^4 (2a\beta)^3} \int_{-\infty}^{\infty} \int_{-\infty}^{\infty} d^2 p d^2 k \\ & \times \frac{1}{(p^2 + \tau^2)(k^2 + \tau^2)[(p+k)^2 + \tau^2]}, \quad (3.2) \\ \Phi(r) &= \frac{\beta c}{(\gamma_1 + \gamma_2)^3} \frac{3(\gamma_1 + \gamma_2)\gamma_1\gamma_2}{(2\pi)^4 (2a\beta)^3} \int_{-\infty}^{\infty} \int_{-\infty}^{\infty} d^2 p d^2 k \\ & \times \frac{e^{i(p+k)r} + e^{-i(p+k)r}}{2(p^2 + \tau^2)(k^2 + \tau^2)[(p+k)^2 + \tau^2]}, \quad (3.3) \end{aligned}$$

where $\tau^2 = b/a$. Substituting Eqs. (2.14) and (3.1) into Eq. (2.4), and referring to our previous calculations for the case where $c=0$ [14], we have

$$\begin{aligned} & \langle \exp\{i q_z [\xi_1(r) - \xi_1(0)]\} \rangle \\ &= e^{-\sigma_1^2 q_z^2} \exp \left\{ q_z^2 \left(\frac{k_B T}{2\pi(\gamma_1 + \gamma_2)} \right) \right. \\ & \left. \times [K_0(\delta r) + (\gamma_2/\gamma_1)K_0(\tau r)] \right\}, \end{aligned} \quad (3.4a)$$

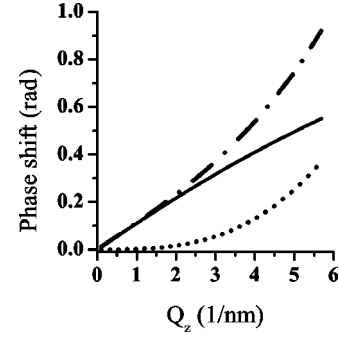


FIG. 3. Phase shift φ for specular reflectivity when $q_{\parallel}=0$ (dashed line), and for longitudinal diffuse scattering when $q_{\parallel}=6 \times 10^{-3} \text{ nm}^{-1}$ (dot-dashed line). The solid line is the difference between the two curves, which represents the relative phase shift between the reflectivity and the diffuse scattering.

$$\begin{aligned} & \langle \exp\{i q_z [\xi_2(r) - \xi_2(0)]\} \rangle \\ &= e^{-\sigma_2^2 q_z^2} \exp \left\{ q_z^2 \left(\frac{k_B T}{2\pi(\gamma_1 + \gamma_2)} \right) \right. \\ & \left. \times [K_0(\delta r) + (\gamma_1/\gamma_2)K_0(\tau r)] \right\}, \end{aligned} \quad (3.4b)$$

$$\begin{aligned} & \langle \exp\{i q_z [\xi_1(r) - \xi_2(0)]\} \rangle \\ &= \exp \left\{ - \left(\frac{\sigma_1^2 + \sigma_2^2}{2} \right) q_z^2 \right\} \exp \left\{ q_z^2 \left(\frac{k_B T}{2\pi(\gamma_1 + \gamma_2)} \right) \right. \\ & \left. \times [K_0(\delta r) - K_0(\tau r)] \right\} \\ & \times [1 - i q_z^3 \Phi_0 - i q_z^3 \Phi(r)], \end{aligned} \quad (3.4c)$$

where σ_1 and σ_2 are the interfacial widths of the two interfaces, and K_0 is the modified Bessel function of order zero. Here, the long wavelength cutoff δ is introduced to represent the effects of gravitation and/or the lateral film size [18,24]. As can be seen from Eq. (2.1), the x-ray scattering is the Fourier transform of the correlation functions. If $c=0$, one gets exactly the same results as in our previous work [14]. However, if $c \neq 0$ the cross-correlation function is complex, suggesting that the interference fringes are not periodic. Namely, there are extra contributions to the phase of the interference terms in Eq. (2.1). The Fourier transform of Φ_0 is a Dirac δ function, i.e.,

$$\begin{aligned} \mathcal{F}\Phi_0 &= \frac{\beta c}{(\gamma_1 + \gamma_2)^3} \frac{\gamma_1^3 + \gamma_2^3}{4\tau^2(2a\beta)^3} \int_0^1 \int_0^1 du dv \\ & \times \frac{1}{1 - v + vu(1 - u)} \delta^2(q_{\parallel}), \end{aligned} \quad (3.5)$$

which leads to a phase shift for both specular and diffuse scattering, proportional to q_z^3 but independent of q_{\parallel} . The Fourier transform of $\Phi(r)$ is

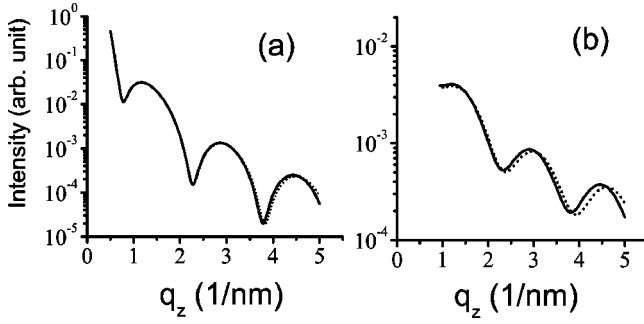


FIG. 4. (a) Comparison between the specular reflectivity when $C=0$ (solid curve) and when $C=6.72 \times 10^{20} \text{ J/m}^5$ (dashed line). (b) Comparison between the longitudinal diffuse scattering when $C=0$ (solid curve) and when $C=6.72 \times 10^{20} \text{ J/m}^5$ (dashed line), calculated for a variation of q_{\parallel} with q_z , as shown in Fig. 2 with $q_{\parallel} = 6 \times 10^{-3} \text{ nm}^{-1}$ at $q_z = 2.5 \text{ nm}^{-1}$.

$$\mathcal{F}\Phi(r) = \frac{\beta c}{(\gamma_1 + \gamma_2)^3} \frac{3(\gamma_1 + \gamma_2)\gamma_1\gamma_2}{4\pi(2a\beta)^3} \times \frac{1}{q_{\parallel}^2 + \tau^2} \int_0^1 \frac{d\alpha}{\alpha(1-\alpha)q_{\parallel}^2 + \tau^2}, \quad (3.6)$$

which, when convoluted with the Fourier transform of the first part on the right-hand side of Eq. (3.4c), leads to an additional phase shift for the diffuse scattering, which depends on both q_z and q_{\parallel} .

IV. NUMERICAL CALCULATIONS

The interference term in Eq. (2.1) can be rewritten as $e^{i(q_z l_m - \varphi)} |\mathcal{F}(e^{iq_z l \xi_1(r) - \xi_2(0)})|$, where φ represents the extra phase shift mentioned above. The Fourier transform $\mathcal{F}(e^{iq_z l \xi_1(r) - \xi_2(0)})$ is calculated numerically. It is a complex function whose argument is φ . The resulting phase shift φ as a function of q_z is shown in Fig. 3. To simulate x-ray scattering from a thin liquid film on top of a liquid subphase, we used the set of parameters in Fig. 1. If $q_{\parallel} = 0$ (for specular reflectivity), φ varies cubically with q_z , namely, $\varphi = \varphi_0 q_z^3$, where φ_0 is calculated according to Eq. (3.5). When $q_{\parallel} \neq 0$, φ becomes $\varphi_0 q_z^3 + \varphi_1(q_{\parallel}, q_z)$. The relative phase shift between the reflectivity and the diffuse scattering, $\varphi_1(q_{\parallel}, q_z)$ varies almost linearly with q_z when q_z is small. If $\sigma_i^2 q_z^2$ is small, one expects that $\varphi_1(q_{\parallel}, q_z)$ depends linearly on q_z [see Eq. (3.4c)]. The deviation from linearity arises mainly from the fact that the correlation function for $c=0$ depends exponentially on q_z^2 . The relative phase shift is also a function of q_{\parallel} . It increases from 0 when $q_{\parallel} = 0$ to a finite value for $q_{\parallel} \neq 0$. The relative phase shift is a direct consequence of the asymmetric nature of the excess free energy of the interface $\Delta G(l)$ and can provide an experimental signature of the anharmonicity of the Hamiltonian.

The reflectivity and diffuse scattering can be calculated numerically from Eq. (2.1). Figure 4(a) shows the comparison between the specular reflection when $c=0$ and when $c \neq 0$. A similar result for the reflectivity has been obtained by Press *et al.* [20,26], who used a cumulant expansion tech-

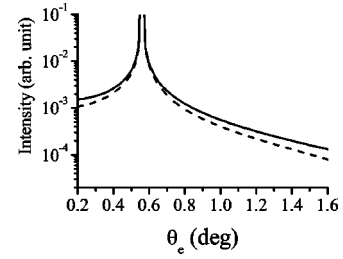


FIG. 5. Comparison between the transverse scattering when $B=0$ (solid curve) and when $B=1.66 \times 10^{11} \text{ J/m}^4$ (dashed lines). The curves run through $q_z = 1.5 \text{ nm}^{-1}$. The wavelength used in the calculation is 0.825 nm . The interfacial tensions are chosen to be $\gamma_1 = 40 \text{ mN/m}$ and $\gamma_2 = 55 \text{ mN/m}$. $T = 300 \text{ K}$.

nique to calculate the phase shift. Figure 4(b) shows the comparison between the longitudinal diffuse scattering when $c=0$ and when $c \neq 0$, calculated for a linear variation of q_{\parallel} with q_z , as shown in Fig. 2 with $q_{\parallel} = 6 \times 10^{-3} \text{ nm}^{-1}$ at $q_z = 2.5 \text{ nm}^{-1}$. In the calculation we assumed that the resolution in the y direction is coarse and, therefore, we integrated out the dependence on the momentum transfer in the corresponding direction q_y . The additional phase shift is observable only at large values of q_{\parallel} .

One can determine the parameter c by measuring the relative phase shift between oscillations in both the reflectivity and the longitudinal diffuse scattering. The parameter b can be determined from the transverse diffuse scattering. If $b=0$, the transverse diffuse scattering is simply the sum of the contributions of the conventional capillary waves of the two interfaces. If $b \neq 0$, one sees a deviation from the conventional capillary wave scattering. If the scanning range is large enough, oscillations appear in the diffuse scattering curves [24]. Figure 5 shows the comparison between the transverse diffuse scattering when $b=0$ and when $b \neq 0$. If $b \neq 0$, the capillary waves on the two interfaces are coupled with a coupling strength proportional to b [14]. Once the two coefficients of the Taylor expansion of the interfacial potential are determined, the interfacial potential itself can be determined by simple algebra [14].

V. CONCLUDING REMARKS

Recent x-ray scattering experiments have measured the resonant diffuse scattering that results from the coupling of capillary waves between two nearby interfaces of thin liquid films [14,24]. These measurements have been interpreted in terms of a quadratic expansion near the minimum of the interfacial free energy (the quadratic term has coefficient b). However, the shape of this minimum is not strictly harmonic, and higher-order terms are expected to be present.

Methods of functional integration and perturbation theory allowed us to evaluate the effect of a small cubic term in the interfacial free energy. This term leads to a complex cross-correlation function with a q_z -dependent variation of the modulation period of the Kiessig fringes. This q_z dependence can be a result of physics other than the cubic term in the interfacial free energy. For example, asymmetry in the time-

averaged density profile across each individual interface may lead to a phase shift in the reflectivity or diffuse scattering [27]. However, our calculation further predicts a phase shift difference between the Kiessig fringes in both the reflectivity and the longitudinal diffuse scattering [i.e., the term $\varphi_1(q_{\parallel}, q_z)$]. This phase shift difference cannot be explained by an asymmetric density profile, and suggests that x-ray scattering can be used to probe the presence of a cubic term in the interfacial free energy. The predicted effects are small, and measurements at large wave vector transfers are required

in order to observe them. Experimental work is in progress to test the theory.

ACKNOWLEDGMENTS

M.L. acknowledges helpful discussions with Professor W.Y. Keung of the University of Illinois at Chicago. This work was supported by a grant to M.L.S. from the National Science Foundation Division of Materials Research (U.S.A.), and by a grant to M.L. from the Chinese Academy of Sciences under the Innovation Program (P. R. China).

-
- [1] I.B. Ivanov, *Thin Liquid Films: Fundamentals and Applications* (Marcel Dekker, New York, 1988).
- [2] B.V. Derjaguin, N.V. Churaev, and V.M. Muller, *Surface Forces* (Consultants Bureau, New York, 1988).
- [3] P.-G. de Gennes, *Rev. Mod. Phys.* **57**, 827 (1985); F. Brochard-Wyart, J.-M. di Meglio, D. Quere, and P.-G. de Gennes, *Langmuir* **7**, 335 (1991).
- [4] A. Sharma and R. Khanna, *Phys. Rev. Lett.* **81**, 3463 (1998).
- [5] S. Dietrich and A. Haase, *Phys. Rep.* **260**, 2 (1995).
- [6] U. Seifert, *Phys. Rev. Lett.* **74**, 5060 (1995).
- [7] K. Ragil, J. Meunier, D. Broseta, J.O. Indekeu, and D. Bonn, *Phys. Rev. Lett.* **77**, 1532 (1996).
- [8] K.J. Mysels and M.N. Jones, *Discuss. Faraday Soc.* **42**, 42 (1966).
- [9] D. Exerowa and A. Scheludko, *C. R. Acad. Bulg. Sci.* **24**, 47 (1971).
- [10] A. Schalchli, J.J. Benattar, and T. Kolarov, *C. R. Acad. Sci., Ser. IIB: Mec., Phys., Chim., Astron.* **319**, 745 (1994).
- [11] D. Bonn and D. Ross, *Rep. Prog. Phys.* **64**, 1085 (2001).
- [12] I.M. Tidswell, T.A. Rabedeau, P.S. Pershan, and S.D. Kosowsky, *Phys. Rev. Lett.* **66**, 2108 (1991).
- [13] J. Wang, M. Tolan, O.H. Seeck, S.K. Sinha, O. Bahr, M.H. Rafailovich, and J. Sokolov, *Phys. Rev. Lett.* **83**, 564 (1999).
- [14] M. Li, A.M. Tikhonov, D.J. Chaiko, and M.L. Schlossman, *Phys. Rev. Lett.* **86**, 5934 (2001).
- [15] D.K. Schwartz, M.L. Schlossman, E.H. Kawamoto, G.J. Kellogg, P.S. Pershan, and B.M. Ocko, *Phys. Rev. A* **41**, 5687 (1990).
- [16] M.K. Sanyal, S.K. Sinha, K.G. Huang, and B.M. Ocko, *Phys. Rev. Lett.* **66**, 628 (1991).
- [17] M.L. Schlossman and P.S. Pershan, in *Light Scattering by Liquid Surfaces and Complementary Techniques*, edited by D. Langevin (Marcel Dekker, New York, 1992), p. 365.
- [18] J.S. Rowlinson and B. Widom, *Molecular Theory of Capillarity* (Clarendon, Oxford, 1982).
- [19] S.K. Sinha, E.B. Sirota, S. Garoff, and H.B. Stanley, *Phys. Rev. B* **38**, 2297 (1988).
- [20] M. Tolan, *X-ray Scattering from Soft-Matter Thin Films*, Springer Tracts in Modern Physics Vol. 148 (Springer, Berlin, 1999).
- [21] M.L. Schlossman, D. Synal, Y. Guan, M. Meron, G. Shea-McCarthy, Z. Huang, A. Acero, S.M. Williams, S.A. Rice, and P.J. Viccaro, *Rev. Sci. Instrum.* **68**, 4372 (1997).
- [22] G. Palasantzas and G. Backx, *Phys. Rev. E* **59**, 1259 (1999).
- [23] J.L. Harden and D. Andelman, *Langmuir* **8**, 2547 (1992).
- [24] J. Daillant and O. Belorgey, *J. Chem. Phys.* **97**, 5837 (1992).
- [25] J. Zinn-Justin, *Quantum Field Theory and Critical Phenomena* (Clarendon, Oxford, 1989).
- [26] W. Press, J.-P. Schlomka, M. Tolan, and B. Asmussen, *J. Appl. Crystallogr.* **30**, 963 (1997).
- [27] L.B. Lurio, T.A. Rabedeau, P.S. Pershan, I.F. Silvera, M. Deutsch, S.D. Kosowsky, and B.M. Ocko, *Phys. Rev. Lett.* **68**, 2628 (1992).